

Effects of radial electric field on ion temperature gradient driven mode stability

Ningfei Chen, Hanyuan Hu, Xiangyu Zhang, Shizhao Wei and Zhiyong Qiu*

Institute for Fusion Theory and Simulation and Department of Physics, Zhejiang University, Hangzhou 310027, China

(Dated: July 3, 2020)

The stability of ion-temperature gradient driven mode (ITG) in the presence of a given radial electric field is investigated using nonlinear gyrokinetic theory. It is found that, radial electric field induced poloidal rotation can significantly stabilize ITG, while the radial electric field induced density perturbation may slightly distort the ITG parallel mode structure, but has little effect on ITG stability.

I. INTRODUCTION

Drift waves (DWs) turbulence [1], driven by free energy associated with plasma pressure gradients, are considered as candidates for inducing anomalous plasma transport and degradation of confinement in magnetically-confined fusion (MCF) devices. Ion-temperature gradient driven mode (ITG) is one of the most intensively studied DWs due to its potential role in causing anomalous ion thermal transport, which is much concerned in future fusion reactors. ITG has two branches, i.e., a slab branch by the coupling of ion parallel compression and diamagnetic drift, and a toroidal branch by the coupling of diamagnetic drift with the unfavored curvature in the weak field side [2, 3]. In-depth understanding of the mechanisms for ITG linear stability, nonlinear evolution and eventual saturation, is needed for quantitative understanding of plasma confinement in future tokamaks. Excitation of zonal flows (ZFs), is considered as an important route for ITG self-regulation, and the regulation is achieved via nonlinear excitation of ZFs by ITG via modulation instability as ITG amplitude exceeds the threshold induced by frequency mismatch, which in turn, scatters ITG into the linearly stable short radial wavelength regime [4, 5].

ZFs are typically meso-scale radial corrugations with toroidally symmetric ($n = 0$), and predominantly poloidally symmetric ($m \simeq 0$) scalar potential fluctuation, and consist of zero-frequency ZF (ZFZF) [6] and its finite frequency counter-part, geodesic acoustic mode (GAM) [5, 7]. Here, m/n are the poloidal/toroidal mode numbers of the torus. The nonlinear interaction of ITG with ZFs are observed in experiments [8–12], and the nonlinear interactions can be confirmed by bi-coherence analysis. The suppression of ITG and the associated transport by self-consistently excited ZFs is observed in large scale simulations [13–16], and it is also found the threshold on pressure gradient on ITG stability is up-shifted as nonlinear effects are taken into account. Furthermore, the radial electric field E_r associated with large-scale mean flow, as well as its gradient, is also observed to be related to turbulence suppression and confinement improvement, and possibly related to the

formation of transport barrier, and transition from low-to high-confinement regime.

ZFs are linearly stable to plasma expansion free energy. However, due to its finite frequency, GAM can resonant with, and be linearly excited by free energy associated with energetic particles (EPs) velocity space anisotropy. This EP-induced GAM (EGAM) is observed in DIII-D experiment with counter-current neutral beam injection [17], and the theoretical interpretation are given based on GAM continuum mode excitation by transit resonance with EPs [18–20]. With the regulation of DW turbulence by ZFs in mind, excitation of EGAM by externally injecting energetic ions into the DW localization region is proposed as a potential active control of DW turbulences [21]. However, recent gyrokinetic simulations show that, after the excitation of EGAM due to EPs injection, the ITG turbulence is instead driven unstable from Dimits shift nonlinearly marginally stable region [22, 23]. These simulation results seem to be contradictory to the speculation based on DW turbulence suppression by ZFs. One possible explanation is that, for the marginally stable ITG in the Dimits shift region, the balanced nonlinearly coupled system [5, 24, 25] will give energy to ITG, as GAM are strongly driven by EPs. Motivated by these simulations, in this work, we will study the nonlinear interaction between ITG and given radial electric field [35] by assuming the time scale separation between ITG and the oscillating electric field, i.e., assuming the ITG frequency and growth rate are both much larger than the electric field oscillating frequency, and study the “linear” stability of ITG in the presence of the radial electric field. This is achieved by deriving an ITG governing mode equation in the existence of the radial electric field induced density modulation as well as poloidal rotation, which is then solved in ballooning space for the ITG local dispersion relation. We note that, the present theory, describes the ITG parallel mode structure and thus, solves for local dispersion relation along the magnetic field lines. Global effects such as E_r -well, and their competition with diamagnetic well in pedestal region of H-mode plasma, will not be included in this local theory, and will be addressed in a future publication. Our model may also shed light on understanding turbulence suppression by mean flow, whose mechanism is not yet fully understood.

The rest of the paper will be organized as follows. In section II, the ITG eigenmode equation in the existence

*E-mail: zqiu@zju.edu.cn

of given radial electric field will be derived using nonlinear gyrokinetic theory. In section III, the ITG stability will be investigated assuming a radial electric field with finite frequency, i.e., that of GAM/EGAM, in both short- and long-wavelength limit. Summary and discussions are given in Section IV.

II. GENERAL FORMALISM

For simplicity of discussion while focusing on the main scope of the present paper, we consider a tokamak with axisymmetric concentric circular magnetic surface and s-straight field line, and a left-handed coordinate (r, θ, ϕ) is adopted, with r , θ and ϕ being the minor radius, poloidal and toroidal angles of the torus, respectively. The equilibrium magnetic field is given as $\mathbf{B} = B_0[(1 - \epsilon \cos \theta)\mathbf{e}_\phi + \epsilon \mathbf{e}_\theta/q]$, where $\epsilon \equiv r/R$ is the inverse aspect ratio, R is the on-axis major radius and $q \equiv rB_\phi/(RB_\theta)$ is the safety factor. ITG generally have ballooning structure with high mode numbers, and the characteristic scale of equilibrium profile is generally much larger than distance between neighbouring mode rational surfaces. Consequently, the perturbed quantity can be expressed as

$$\delta\phi = e^{in\phi - i\omega t} \sum_j \hat{\Phi}(s - j) e^{-i(m_0 + j)\theta}. \quad (1)$$

Here, $s \equiv (r - r_0)/\Delta r = nq - m_0$, r_0 denotes the reference rational surface with $nq(r_0) - m_0 = 0$, $\Delta r = 1/(n\partial q/\partial r)$ is the distance between neighboring mode rational surfaces, and $|j| \ll m_0$ is an integer.

The nonlinear gyrokinetic equation [26] is used to investigate the interaction between ITG turbulence and the given radial electric field. Following Ref. [3], we take the flat density gradient limit to focus on effects of ion temperature gradient, i.e., assuming $\eta_i = L_{ni}/L_{Ti} \rightarrow \infty$, with $L_{ni} = -n_i/(\partial n_i/\partial r)$ and $L_{Ti} = -T_i/(\partial T_i/\partial r)$ being the characteristic scale length of ion density and temperature nonuniformity, respectively. Note that the frequency of the radial electric field is generally much lower than the frequency and growth rate of ITG turbulence, so the slow time-dependence of E_r can be neglected compared to fast ITG time scale. The validity of this assumption will be verified *a posteriori*. The nonlinear gyrokinetic equation for ion response to ITG can be written as

$$\begin{aligned} (\omega - k_\parallel v_\parallel + \omega_D) \delta H_I &= \frac{e}{T_i} J_0 (\omega + \omega_{*i}^T) F_{0i} \delta\phi_I \\ &\quad - \Lambda J_{\mathbf{k}'} \delta H_{\mathbf{k}''} \delta\phi_{\mathbf{k}'}. \end{aligned} \quad (2)$$

Here, $k_\parallel \equiv (nq - m)/(qR)$ is the parallel wavenumber, $\omega_D \equiv 2\omega_d C (x_\perp^2/2 + x_\parallel^2)$ is the magnetic drift frequency, with $\omega_d = k_\theta c T_i / (eBR)$, $x_\perp = v_\perp/v_{ti}$ and $x_\parallel = v_\parallel/v_{ti}$ being the ion perpendicular/parallel velocities normalized by thermal velocity $v_{ti} = \sqrt{2T_i/m_i}$, respectively. $C = \cos \theta - k_r \sin \theta/k_\theta$ is related to the curvature with k_r

and $k_\theta = m_0/r_0$ being the radial/poloidal mode numbers. δH_I is the nonadiabatic ion response to ITG, $J_0(k_\perp \rho_i)$ is the Bessel function of zero-index accounting for Finite Larmor radius (FLR) effects, $\rho_s = mv_{\perp,s}c/(eB)$ is the Larmor radius of species s , F_{0i} is the equilibrium ion distribution function, and $\omega_{*i}^T = \omega_{*Ti} (x_\perp^2 + x_\parallel^2 - 3/2)$ is the ion diamagnetic frequency in the flat density limit, with $\omega_{*Ti} = k_\theta c T_i / (eBL_{Ti})$. Furthermore, the second term on the right hand side of Eq. (2) is the formal nonlinear term, where $\Lambda \equiv i(c/B_0) \sum_{\mathbf{k}=\mathbf{k}'+\mathbf{k}''} \mathbf{b} \cdot (\mathbf{k}'' \times \mathbf{k}')$, and other notations are standard. It is noteworthy that there are two nonlinear terms, i.e., radial electric field induced poloidal rotation of ITG $\propto \delta\phi_E \delta H_I$ and periodicity along the magnetic field line induced by density perturbation associated with the radial electric field $\propto \delta\phi_I \delta H_E$. Here, subscripts ‘‘E’’ and ‘‘I’’ represent quantities associated with radial electric field and ITG, respectively. The dispersion equation can be derived from charge quasi-neutrality condition

$$\frac{eN_0\delta\phi}{T_e} + \langle \delta H_e J_0 \rangle = -\frac{eN_0\delta\phi}{T_i} + \langle \delta H_i J_0 \rangle, \quad (3)$$

with $eN_0\delta\phi/T_e$ and $-eN_0\delta\phi/T_i$ being adiabatic responses of electron and ion, respectively, and $\langle \dots \rangle$ representing velocity space integration. The derivation follows closely the procedure of Ref. [27]. For typical ITG fluctuation with $k_\parallel v_{\parallel,e} \gg \omega \sim \omega_{*i} \gg \omega_d$, $k_\parallel v_{\parallel,i}$, electrons responde adiabatically, i.e., $\delta H_{I,e} = 0$. The nonadiabatic ion response can be derived as

$$\begin{aligned} \delta H_{I,i} &\approx \frac{\Lambda}{\omega} \left[-\left(\frac{e}{T_e} + \frac{e}{T_i} \right) F_0 \delta\phi_E + \delta H_E \right] \delta\phi_I \\ &+ \frac{e}{T_i} J_0 F_0 \left(1 + \frac{\omega_{*i}^T}{\omega} \right) \left(1 + \frac{k_\parallel v_\parallel}{\omega} + \frac{k_\parallel^2 v_\parallel^2}{\omega^2} - \frac{\omega_D}{\omega} \right) \delta\phi_I. \end{aligned} \quad (4)$$

The two terms in first bracket of Eq. (4) are the formal nonlinear terms, and represent the effects associated with potential and density fluctuation of E_r , respectively. Quasi-neutrality condition of ITG is applied to simplify the first term. Substituting the ion and electron response into quasi-neutrality condition (3), one then have the ITG WKB dispersion relation

$$\begin{aligned} &\left\{ \frac{1}{\tau(1 + \omega_{*Ti}/\omega)} + b_\perp - \frac{k_\parallel^2 v_{ti}^2}{2\omega^2} + \frac{2\omega_d C}{\omega} + \frac{\Lambda}{\omega + \omega_{*Ti}} \right. \\ &\quad \left. \times \left[\left(1 + \frac{1}{\tau} \right) \delta\phi_E - \frac{T_i}{e} \left\langle \frac{\delta H_{E,i}}{N_0} \right\rangle \right] \right\} \delta\phi = 0, \end{aligned} \quad (5)$$

with $b_\perp \equiv k_\perp^2 \rho_i^2/2$, and k_\perp being the perpendicular wavenumber. The first four terms of Eq. (5) constitute the linear ITG dispersion relation, with the first three terms being respectively, adiabatic electron response, the FLR effect (polarization) and parallel compressibility, while the forth term related to magnetic drift peculiar in toroidal configuration, resulting in coupling of neighbouring poloidal harmonics. The last two terms are nonlinear modifications due to poloidal rotation and density

modulation associated with the radial electric field, respectively. Noting $k_{\perp}^2 = k_{\theta}^2 - \partial^2/\partial r^2$, the eigenmode equation in real space for j -th poloidal harmonics can be derived as

$$\begin{aligned} & \left(b_{\theta} \hat{s}^2 \frac{d^2}{dz^2} - \frac{1}{\tau(1 + \omega_{*T_i}/\omega)} - b_{\theta} + \frac{k_{\parallel}^2 v_{Ti}^2}{2\omega^2} \right) \hat{\Phi}_z \\ &= \frac{\omega_d}{\omega} \left[\hat{\Phi}_{z+1} + \hat{\Phi}_{z-1} + \hat{s} \frac{d}{dz} (\hat{\Phi}_{z+1} - \hat{\Phi}_{z-1}) \right] \\ &+ \frac{\Lambda}{(\omega + \omega_{*T_i})} \left[\left(1 + \frac{1}{\tau} \right) \delta\phi_E - \left\langle \frac{T_i \delta H_{E,i}}{eN_0} \right\rangle \right] \hat{\Phi}_z. \quad (6) \end{aligned}$$

Here, $\hat{s} \equiv r(\partial q/\partial r)/q$ is the magnetic shear, $\tau \equiv T_e/T_i$, $b_{\theta} \equiv k_{\theta}^2 \rho_{Ti}^2/2$, $z \equiv s - j = nq - m$ is the normalized distance to the mode rational surface. The first term on the right-hand side of Eq (6) comes from the curvature drift induced coupling between neighbouring poloidal harmonics. Moreover, the term proportional to $\langle \delta H_{E,i} \rangle$ may also have poloidal-dependence, and causes additional toroidal coupling. For instance, GAM with $\omega \gg \omega_{tr,i}$, is characterised by up-down anti-symmetric ($\propto \sin \theta$) density fluctuation, while ZFZF with $\omega \ll \omega_{tr,i}$, has $\cos \theta$ -type density fluctuation. Here $\omega_{tr,i} \equiv v_{\parallel,i}/(qR)$ is the circulating ion transit frequency. Eq. (6) can be analyzed using the ballooning mode formalism framework [28], which is accomplished by taking $\Phi(\eta) = \int \hat{\Phi}(z) \exp(-i\eta z) dz$, with η being the extended poloidal angle along the magnetic field lines. The ITG eigenmode equation in ballooning space reads

$$\begin{aligned} & \frac{d^2 \Phi(\eta)}{d\eta^2} + q^2 \Omega^2 b \left(\frac{\tau \Omega}{1 + \tau \Omega \epsilon_{Ti}^{1/2}} + b(1 + \hat{s}^2 \eta^2) \right) \\ &+ \frac{2}{\Omega} (\cos \eta + \hat{s} \eta \sin \eta) + (1 + \tau) \Delta_E \delta\phi_E \\ &- \tau \Delta_E \left\langle \frac{T_i \delta H_{E,i}}{eN_0} \right\rangle \Phi(\eta) = 0, \quad (7) \end{aligned}$$

where $\Omega \equiv \omega/(\tau \sqrt{\omega_{*T_i} \omega_d})$, $b \equiv \tau b_{\theta}/\sqrt{\epsilon_{Ti}}$, $\epsilon_{Ti} \equiv L_{Ti}/R$ and $\Delta_E \equiv \Lambda/[\omega_{*T_i} \sqrt{\epsilon_{Ti}} (1 + \tau \Omega \sqrt{\epsilon_{Ti}})]$. Eq. (7) is general and can be applied to study the nonlinear modification of any given radial electric field to ITG stability, with the nonlinear modifications accounted for by the last two terms. In this work, as a proof of principle demonstration, we will consider GAM/EGAM-like oscillations with finite frequency, while the effects of ZFZF can be investigated straightforwardly following the same approach. Since this is a local model describing the parallel mode structure along the magnetic field lines, the global radial envelope of EGAM is not taken into account. It is natural to take the dominant $m = 0, 1$ components of nonadiabatic ion response $\delta H_{E,i}$ [29]

$$\delta H_{E,i} = \frac{eF_0 \overline{\delta\phi_E}}{T_i} \left[1 - \frac{\omega_{Dr}}{\omega_G} \left(\frac{x_{\perp}^2}{2} + x_{\parallel}^2 + \tau \right) \right], \quad (8)$$

and $m = 0$ component of $\delta\phi_E$, i.e., $\overline{\delta\phi_E}$, where $(\overline{\dots}) \equiv \int_0^{2\pi} (\dots) d\theta/2\pi$ represents surface averaged quantity. The

higher order $m = 1$ density perturbation of GAM/EGAM is included, to account for its unique role in inducing periodic modification to the ITG eigenmode potential well along the magnetic field line, that determines the condition for ITG stability. Here, $\omega_G = \sqrt{7/4 + \tau v_{Ti}/R_0}$ is the real frequency of GAM, $\omega_{Dr} = 2\omega_{dr} \sin \theta$ is the magnetic drift frequency associated with geodesic curvature, with $\omega_{dr} \equiv k_r c T_i / (eBR)$.

III. EFFECTS OF E_r ON ITG LINEAR STABILITY

With specified expression of $\delta H_{E,i}$ presented in Eq. (8), Eq. (7) can be written as

$$\begin{aligned} & \frac{d^2 \Phi}{d\eta^2} + q^2 \Omega^2 b \left(\frac{\tau \Omega}{1 + \tau \Omega \epsilon_{Ti}^{1/2}} + b(1 + \hat{s}^2 \eta^2) + \Delta_E \overline{\delta\phi_E} \right) \\ &+ \frac{2}{\Omega} (\cos \eta + \hat{s} \eta \sin \eta) + \Delta'_E \overline{\delta\phi_E} \sin \eta \Phi = 0, \quad (9) \end{aligned}$$

where $\Delta_E \overline{\delta\phi_E}$ represents modification due to the electrostatic potential, and $\Delta'_E \overline{\delta\phi_E} \sin \eta$ is originated from the $m = 1$ density perturbation of EGAM, with $\Delta'_E \equiv (2\omega_{dr}/\omega_G) \tau (1 + \tau) \Delta_E$.

A. Short-wavelength limit

In the short-wavelength limit, i.e., $b \sim O(1)$, the eigenfunction is localized in ballooning space [3]. Thus, strong coupling approximation can be adopted by taking $\cos \eta \approx 1 - \eta^2/2$ and $\sin \eta \approx \eta$ [30]. Note that, the assumption underlying the above strong coupling approximation is that the mode is localized around $\eta = 0$, which is not necessarily the case as clearly shown by the shift $\Delta\eta$ as discussed below in Eq. (10). However, as we show in Fig. 3, the mode structure shift $\Delta\eta$ is quite small, the above assumption is still valid. The eigenmode equation then becomes

$$\begin{aligned} & \frac{d^2 \Phi}{d\eta^2} + q^2 \Omega^2 b \left(\frac{\tau \Omega}{1 + \tau \Omega \epsilon_{Ti}^{1/2}} + b + \frac{2}{\Omega} + \Delta_E \overline{\delta\phi_E} \right) \\ &+ \left(b\hat{s}^2 + \frac{2\hat{s} - 1}{\Omega} \right) \eta^2 + \Delta'_E \overline{\delta\phi_E} \eta \Phi = 0, \quad (10) \end{aligned}$$

which can be rewritten as a standard Weber equation by taking $\eta' = \eta + \Delta\eta$, with $\Delta\eta = \Delta'_E \overline{\delta\phi_E} / (2b\hat{s}^2 + 2(2\hat{s} - 1)/\Omega)$ representing the mode shift from the unfavourable curvature region. The most unstable ground eigenmode is given by $\delta\phi = \exp(-\sigma(\eta + \Delta\eta)^2)$ with

$$\begin{aligned} \sigma &= \frac{q^2}{2} \left(\frac{\tau b \Omega^3}{1 + \tau \Omega \epsilon_{Ti}^{1/2}} + 2b\Omega + b^2 \Omega^2 \right) \\ &+ \frac{q^2 \Omega^2 b}{2} \left(\Delta_E \overline{\delta\phi_E} - \frac{(\Delta'_E \overline{\delta\phi_E})^2}{4(b\hat{s}^2 + (2\hat{s} - 1)/\Omega)} \right). \end{aligned}$$

The half width of the eigenmode in η space is proportional to $1/b$. The corresponding dispersion relation is

$$q^2\Omega^2b \left[\frac{\tau\Omega}{1 + \tau\Omega\epsilon_{Ti}^{1/2}} + \frac{2}{\Omega} + b + \Delta_E\overline{\delta\phi_E} - \frac{(\Delta'_E\overline{\delta\phi_E})^2}{4(b\hat{s}^2 + (2\hat{s} - 1)/\Omega)} \right]^2 + \left(b\hat{s}^2 + \frac{2\hat{s} - 1}{\Omega} \right) = 0. \quad (11)$$

The dispersion relation is similar to corresponding linear result [3], except the last two terms in the square bracket from the contribution of radial electric field induced poloidal rotation and density fluctuation, respectively. The dependence of ITG growth rate and real frequency on the radial electric field are solved from the analytical dispersion relation (11), which are then compared with the numerical solution of Eq. (9), and good agreement between analytical and numerical results are obtained, as shown in Fig. 1a and 1b, respectively. The ITG growth rate decreases significantly with increasing $\delta\phi_E$. We then analyze the contribution of the radial electric field induced poloidal rotation and density modulation on ITG stability, by turning off the corresponding terms in Eq. (9). It is shown in Fig. 2 that, when the E_r induced poloidal rotation is kept while the density perturbation is turned off, the ITG growth rate is almost the same as that with both effects properly accounted for; while as only the E_r induced density perturbation is kept, the ITG growth rate is almost independent of the scalar potential. We thus conclude that the reduction of the growth rate is mainly due to the potential fluctuation (poloidal rotation). In addition, it is found that the ITG growth rate is of order C_s/L_T , which is much larger than GAM/EGAM frequency $\sim C_s/R$, hence our analysis, by assuming GAM/EGAM frequency is much smaller than ITG frequency and growth rate, is self-consistent. The mode structure is also shown in Fig. 3, and it is clearly seen that the peak of the mode structure shifts away from $\eta = 0$ and the even symmetry is slightly broken, resulting from the odd modification to the potential well introduced by the density fluctuation of finite frequency E_r ($\propto \sin\theta$) as denoted by Δ'_E . We note that, Eq. (9) can be further simplified, by substituting the quasi-neutrality condition of GAM/EGAM into Eq. (7) to replace the last term proportional to $\langle\delta H_{E,i}\rangle$. This process will introduce $O(k_r^2\rho_i^2)$ uncertainty since it is $\langle J_0\delta H_{E,i}\rangle$ in the quasi-neutrality condition instead of the $\langle\delta H_{E,i}\rangle$ in Eq. (7). In this case, the obtained ITG eigenmode equation will be even in η . One can then conclude the symmetry breaking induced by the density modulation finite frequency radial electric field cannot be larger than $O(k_r^2\rho_i^2)$, and is thus weak, as shown by our numerical results.

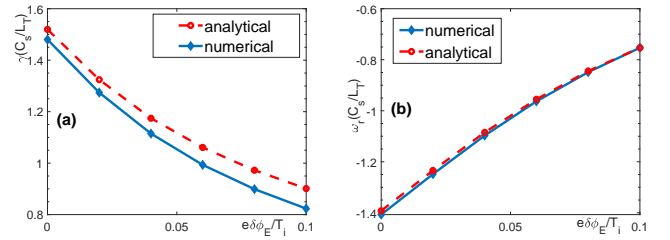


FIG. 1: The dependence of normalized growth rate (a) and real frequency (b) of ITG, which are normalized by C_s/L_{Ti} , on the normalized EGAM/GAM intensity $e\delta\phi_E/T_i$. The circles represent the analytical result given by Eq. (11) while diamonds are numerical result of Eq. (9). Here, $C_s^2 \equiv 2T_e/m_i$ is the sound speed, $\epsilon_{Ti} = 0.2$ and $b = 1$.

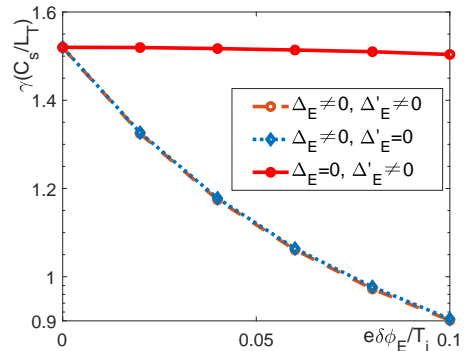


FIG. 2: Analytical result of integrated and separated effects of potential and density fluctuation of GAM/EGAM.

B. Long-wavelength limit

For typical tokamak plasmas, strong coupling approximation is usually a crude constraint. In more general cases, $b \ll 1$ (long-wavelength limit) is satisfied, and strong coupling approximation no longer holds. In the long-wavelength limit, there are two branches, i.e., toroidal branch and slab branch. We are more concerned about the toroidal branch [3], which is characterized by fast variation over connection length scale ($\eta \sim O(1)$) and a superimposed slowly varying envelope over secular scale. The self-consistent ordering is given by balancing parallel compressibility and adiabatic electron response, which results in $\Omega = O(b^{-1/3})$. Taking $\Phi(\eta) = C_0(\eta_1)\cos\eta/2 + S_0(\eta_1)\sin\eta/2$ with $\eta_1 \equiv \hat{\epsilon}\eta$, and $\hat{\epsilon} = b^{1/3}$ denoting slow variation in η , the eigenmode equations can be derived from vanishing coefficients of

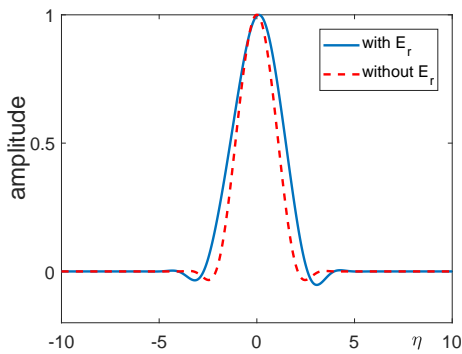


FIG. 3: The mode structure of the lowest eigenmode when $e\delta\phi_E/T_i = 0.1$. Here, $\epsilon_{Ti} = 0.2$, $b = 1$.

$\sin \eta/2$ and $\cos \eta/2$:

$$\frac{dS_0}{d\eta_1} + \left(\frac{b^{2/3}q^2\Omega^3\tau}{1 + \tau\Omega\epsilon_{Ti}^{1/2}} - \frac{1}{4b^{1/3}} + q^2\Omega^2b^{2/3}\Delta_E\overline{\delta\phi_E} \right) C_0 + q^2\Omega b^{1/3}\hat{s}\eta_1 S_0 + \frac{1}{2}q^2\Omega^2b^{2/3}\Delta'_E\overline{\delta\phi_E} S_0 = 0, \quad (12)$$

$$\frac{dC_0}{d\eta_1} - \left(\frac{b^{2/3}q^2\Omega^3\tau}{1 + \tau\Omega\epsilon_{Ti}^{1/2}} - \frac{1}{4b^{1/3}} + q^2\Omega^2b^{2/3}\Delta_E\overline{\delta\phi_E} \right) S_0 - q^2\Omega b^{1/3}\hat{s}\eta_1 C_0 - \frac{1}{2}q^2\Omega^2b^{2/3}\Delta'_E\overline{\delta\phi_E} C_0 = 0. \quad (13)$$

Equations (12) and (13) can be cast into a Weber equation for C_0 and S_0 by taking $\eta' = \eta + b^{1/3}\Delta_E\overline{\delta\phi_E}/2\hat{s}$. The dispersion relation for the most unstable ground eigenstate is

$$\Omega^3 + \frac{\Lambda\overline{\delta\phi_E}}{\tau\omega_{*T}\epsilon_{Ti}^{1/2}}\Omega^2 - \frac{\epsilon_{Ti}^{1/2}}{4bq^2}\Omega = \frac{1}{4bq^2\tau}. \quad (14)$$

Here, the second term of Eq. (14) comes from the $m = 0$ component of radial electric field induced poloidal rotation, and other terms originate from linear dispersion relation [3]. It is noteworthy that the $m = 1$ component of density perturbation has no influence on the dispersion relation, possibly due to the wideness of mode structure in η space (shown in Fig. 6), and the $m = 1$ density fluctuation is averaged out due to its fast variation along the magnetic field lines. The dependence of ITG growth rate and real frequency on scalar potential of the radial electric field are solved from the analytical dispersion relation, which are then compared with the numerical solution of Eq. (9), and good agreement are obtained, as shown in Fig. 4. An artificially small $b = 0.01$ is adopted to separate different scales. As shown in Fig. 5, the E_r induced poloidal rotation is the sole reason for the reduction of the ITG growth rate, as clarified by our theoretical analysis; while its density perturbation has little effects on ITG stability. There is also angle shift in the mode structure from the unfavorable curvature region as shown in Fig. 6, but it is less obvious than that in the short-wavelength limit.

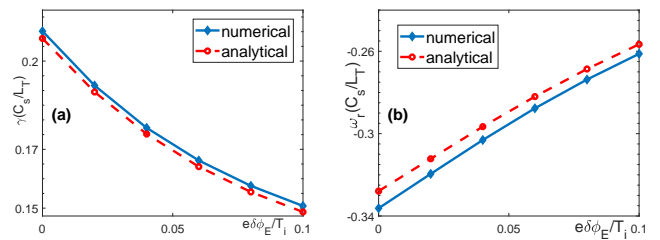


FIG. 4: The growth rate (a) and real frequency (b) of ITG versus the normalized EGAM/GAM intensity $e\delta\phi_E/T_i$. The circles represent the analytical result given by Eq. (14) while diamonds represent numerical result of Eq. (9). Here, $\epsilon_{Ti} = 0.2$, $b = 0.01$.

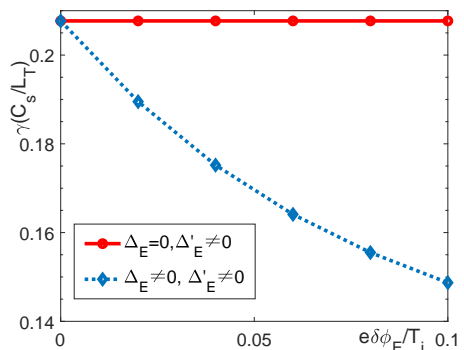


FIG. 5: Analytical result of integrated and separated effects of GAM/EGAM potential and density fluctuation. The result of retaining only potential fluctuation is exactly the same as that of retaining both effects.

IV. CONCLUSION AND DISCUSSION

In this paper, a governing equation is formulated to investigate the ITG “linear” stability in the presence of a given radial electric field, using nonlinear gyrokinetic equation and ballooning mode representation. The effects of the radial electric field on ITG linear stability consist of E_r -induced poloidal rotation and density fluctuation, and their respective contribution to ITG stability are studied both analytically and numerically.

For typical tokamak parameters, the frequency of E_r is much lower than the time scale of ITG turbulence, and thus, it is treated as static equilibrium. For the adopted GAM/EGAM-like radial electric field with $\omega \gg \omega_{tr,i}$, we found that the poloidal rotation is the main reason for the significant reduction of the ITG growth rate in short-wavelength limit and the sole reason in the long-wavelength limit. On the contrary, the up-down anti-symmetric density perturbation have little suppression effect on ITG turbulence in both short- and long-wavelength limit, which may be resulted from the

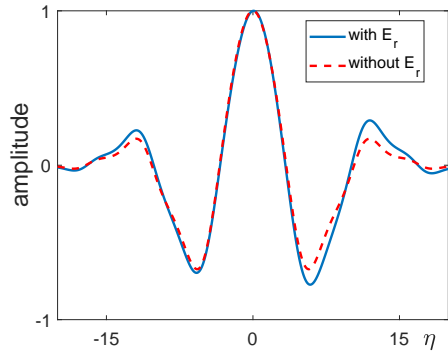


FIG. 6: The mode structure of the most unstable mode when $e\delta\phi_E/T_i = 0.1$. Here, $\epsilon_{Ti} = 0.2$, $b = 0.01$.

poloidally up-down anti-symmetric ($\propto \sin\theta$) density perturbation vanishes in the unfavourable curvature region where ITG localizes. The density perturbation causes the mode structure shift in the extended poloidal angle, due to the finite frequency radial electric field induced $\sin\eta$ -type density modulation that breaks the even symmetry of the potential well, though this symmetry breaking is weak by $O(k_r^2\rho_i^2)$. The extension to the stability of ITG in the presence of ZFZF or mean flow with frequency much lower than ion transit frequency, and thus, up-down symmetric density perturbation ($\propto \cos\theta$), is straightforward. It is found that, the radial electric field induced poloidal

rotation will significantly stabilize ITG; while the density perturbation, though overlapping with the ITG localization, plays secondary role, as in the GAM/EGAM case investigated in the present work.

The present work, motivated to understand the numerically observed “excitation” of ITG in the Dimits shift region by EGAM, found instead that, the radial electric field always play stabilizing role on ITG. Potential effects that may modify the present picture based on local ITG linear stability in the presence of a given radial electric field, and interpret the numerical results of Ref. [22, 23], include 1. modification of ITG radial envelope [31] by the typically radially global mode structure of EGAM and 2. the transient suppression of the ZF radial electric field existing in the Dimits shift region as the excited EGAM has opposite phase. These effects will be investigated in a future work.

Acknowledgements

This work is supported by the National Key R&D Program of China under Grant No. 2017YFE0301900, and the National Science Foundation of China under grant No. 11875233. The original idea of investigating ITG stability in the existence of EGAM induced periodic modification to the potential well was provided by Prof. Liu Chen (Zhejiang University and University of California, Irvine).

-
- [1] W. Horton, *Rev. Mod. Phys.* **71**, 735 (1999).
[2] C. Z. Cheng and L. Chen, *The Physics of Fluids* **23**, 1770 (1980).
[3] L. Chen, S. Briguglio, and F. Romanelli, *Physics of Fluids B: Plasma Physics* **3**, 611 (1991).
[4] L. Chen, Z. Lin, and R. White, *Physics of Plasmas* **7**, 3129 (2000).
[5] F. Zonca and L. Chen, *EPL (Europhysics Letters)* **83**, 35001 (2008).
[6] P. H. Diamond, S.-I. Itoh, K. Itoh, and T. S. Hahm, *Plasma Physics and Controlled Fusion* **47**, R35 (2005).
[7] N. Winsor, J. L. Johnson, and J. M. Dawson, *The Physics of Fluids* **11**, 2448 (1968).
[8] K. J. Zhao, T. Lan, J. Q. Dong, L. W. Yan, W. Y. Hong, C. X. Yu, A. D. Liu, J. Qian, J. Cheng, D. L. Yu, et al., *Phys. Rev. Lett.* **96**, 255004 (2006).
[9] G. D. Conway, C. Troster, B. Scott, K. Hallatschek, and the ASDEX Upgrade Team, *Plasma Physics and Controlled Fusion* **50**, 055009 (2008).
[10] T. Lan, A. D. Liu, C. X. Yu, L. W. Yan, W. Y. Hong, K. J. Zhao, J. Q. Dong, J. Qian, J. Cheng, D. L. Yu, et al., *Physics of Plasmas* **15**, 056105 (2008).
[11] W. Zhong, Z. Shi, Y. Xu, X. Zou, X. Duan, W. Chen, M. Jiang, Z. Yang, B. Zhang, P. Shi, et al., *Nuclear Fusion* **55**, 113005 (2015).
[12] A. Melnikov, L. Eliseev, S. Lysenko, M. Ufimtsev, and V. Zenin, *Nuclear Fusion* **57**, 115001 (2017).
[13] Z. Lin, T. S. Hahm, W. W. Lee, W. M. Tang, and R. B. White, *Science* **281**, 1835 (1998).
[14] T. S. Hahm, K. H. Burrell, Z. Lin, R. Nazikian, and E. J. Synakowski, *Plasma Physics and Controlled Fusion* **42**, A205 (2000).
[15] F. Liu, Z. Lin, J. Q. Dong, and K. J. Zhao, *Physics of Plasmas* **17**, 112318 (2010).
[16] X. Liao, Z. Lin, I. Holod, B. Li, and G. Y. Sun, *Physics of Plasmas* **23**, 122305 (2016).
[17] R. Nazikian, G. Y. Fu, M. E. Austin, H. L. Berk, R. V. Budny, N. N. Gorelenkov, W. W. Heidbrink, C. T. Holcomb, G. J. Kramer, G. R. McKee, et al., *Phys. Rev. Lett.* **101**, 185001 (2008).
[18] G. Y. Fu, *Phys. Rev. Lett.* **101**, 185002 (2008).
[19] Z. Qiu, F. Zonca, and L. Chen, *Plasma Physics and Controlled Fusion* **52**, 095003 (2010).
[20] H. Berk and T. Zhou, *Nuclear Fusion* **50**, 035007 (2010).
[21] Z. Qiu, L. Chen, and F. Zonca, *Plasma Science and Technology* **20**, 094004 (2018).
[22] D. Zarzoso, Y. Sarazin, X. Garbet, R. Dumont, A. Strugarek, J. Abiteboul, T. Cartier-Michaud, G. Dif-Pradalier, P. Ghendrih, V. Grandgirard, et al., *Phys. Rev. Lett.* **110**, 125002 (2013).
[23] R. J. Dumont, D. Zarzoso, Y. Sarazin, X. Garbet, A. Strugarek, J. Abiteboul, T. Cartier-Michaud, G. Dif-Pradalier, P. Ghendrih, J.-B. Girardo, et al., *Plasma Physics and Controlled Fusion* **55**, 124012 (2013).
[24] Z. Qiu, L. Chen, and F. Zonca, *Physics of Plasmas* **21**, 022304 (2014).

- [25] Z. Qiu, L. Chen, and F. Zonca, *Physics of Plasmas* **22**, 042512 (2015).
- [26] E. A. Frieman and L. Chen, *The Physics of Fluids* **25**, 502 (1982).
- [27] P. N. Guzdar, L. Chen, W. M. Tang, and P. H. Rutherford, *The Physics of Fluids* **26**, 673 (1983).
- [28] J. Connor, R. Hastie, and J. Taylor, *Proceedings of the Royal Society of London series a-mathematical physical and engineering sciences* **365**, 1 (1979).
- [29] Z. Qiu, L. Chen, and F. Zonca, *Plasma Physics and Controlled Fusion* **51**, 012001 (2008).
- [30] J. Taylor, *Plasma Physics and Controlled Nuclear Fusion Research* **2**, 323 (1976).
- [31] F. Romanelli and F. Zonca, *Physics of Fluids B: Plasma Physics* **5**, 4081 (1993).
- [32] L. Chen and F. Zonca, *Phys. Rev. Lett.* **109**, 145002 (2012).
- [33] Z. Qiu, L. Chen, and F. Zonca, *Nuclear Fusion* **57**, 056017 (2017).
- [34] A. Biancalani, A. Bottino, A. D. Siena, F. Jenko, P. Lauber, A. Mishchenko, I. Novikau, and L. Villard, submitted to *Plasma Physics and Controlled Fusion* (2020).
- [35] For “given” radial electric field, we refer to radial electric field that is not generated by the DW itself. Thus, it can include EGAM, mean flow and, ZF generated by other kinds of turbulence such as Alfvén eigenmodes. [32–34]